

The Dehydration Step in the Enzyme-Coenzyme-B₁₂ Catalyzed Diol Dehydrase Reaction of 1,2-Dihydroxyethane Utilizing a Hydrogen-Bonded Carboxylic Acid Group as an Additional Cofactor: A Computational Study

Philip George,[†] Per E. M. Siegbahn,[‡] Jenny P. Glusker,^{*,†} and Charles W. Bock^{†,§}

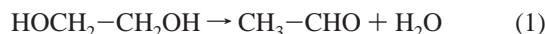
The Institute for Cancer Research, Fox Chase Cancer Center, 7701 Burholme Avenue, Philadelphia, Pennsylvania 19111, Department of Physics, University of Stockholm, Sweden, and Department of Chemistry, Philadelphia University, Henry Avenue and School House Lane, Philadelphia, Pennsylvania 19144

Received: April 20, 1999; In Final Form: June 14, 1999

The various steps in a mechanism for the diol dehydrase reaction in which a carboxylic acid group of an amino acid residue at the active site of the enzyme serves as an additional cofactor have been investigated using density functional theory (B3LYP) calculations. This mechanism involves a neutral radical rather than a protonated radical (radical cation). 1,2-Dihydroxyethane was chosen as the substrate, and formic acid was selected as a model for the carboxylic acid group. The 1,2-dihydroxyeth-1-yl radical (produced by H-atom transfer from the substrate to the 5'-deoxyadenosyl radical) forms a nine-membered ring structure with the formic acid. There are two intermolecular hydrogen bonds in this ring structure—one with the OH of the $\dot{\text{C}}\text{-OH}$ group in the radical as a hydrogen donor and the C=O group in the formic acid as an acceptor, and the other with the OH of the C—OH group in the radical as an acceptor and the C—OH group of the formic acid as a hydrogen donor. Bond rearrangement within this hydrogen-bonded ring structure results in the formation of a hydrogen-bonded product in which transfer of the radical center from one carbon atom to the adjacent carbon atom has taken place. Fission of the C—O bond at the new radical center leads to the elimination of H₂O and the separation of the formylmethyl radical from which acetaldehyde is formed by H-atom transfer. The interchange of the HO—C and C=O bonding in the carboxylic acid group is an overall feature of the mechanism. Furthermore, like the radical, the substrate diol is found to form a nine-membered ring structure with formic acid; this contains two intermolecular hydrogen bonds analogous to those formed between the radical and formic acid. This finding provides support for the hypothesis that two-point attachment of the substrate via its HO groups to the enzyme occurs prior to the H-atom transfer, which initiates the dehydration process. Geometries, energies, and entropies are reported for the hydrogen-bonded reactant ring structure, for the transition state, for a hydrogen-bonded product structure, and for all the separate molecules. Enthalpy, entropy, and free energy changes for the various steps have been calculated from these data, which relate to the gas phase, and for the corresponding reactions at the active site where the restricted spatial environment results in a much diminished translational entropy. Modified entropy values have accordingly been employed by taking the liquid state as the model, evaluating S_{liq}^{298} using the empirical equation, $S_{\text{liq}}^{298} = S_{\text{internal}}^{298} + 15.8$. Further calculations suggest that polarization within the protein cavity containing the active site has a very small effect on the barrier height and the exothermicity of the dehydration process. Rate constants calculated from computed free energies of activation for the dehydration via an HO-bridge structure (transition state), and via fragmentation giving the HO-radical and *syn*-vinyl alcohol, are far smaller than the experimentally determined rate constant, whereas that calculated for the formic acid cofactor mechanism is of the same order of magnitude as the experimental value.

Introduction

In the enzyme-coenzyme B₁₂ catalyzed dehydration of 1,2-dihydroxyethane,



homolytic fission of the AdoCH₂—Co^{III} bond in 5'-deoxyadenosylcobalamin produces the AdoCH₂[•] radical and Co^{II}.

Reaction of this radical with the diol substrate generates the 1,2-dihydroxyeth-1-yl radical, HOCH₂— $\dot{\text{C}}\text{HOH}$, and subsequent reactions lead to the formation of the acetaldehyde and water. The mechanism by which this comes about, whether by the transfer of an HO group from one carbon atom to the other followed by the elimination of H₂O from the 1,1-diol, or in some other way, has been studied experimentally, notably using isotopic labeling^{1a,c,d,f} and model catalysts,^{1c,h} and has been the subject of many review articles.^{1a,b,g,i,j}

Besides radical species, protonated radicals (radical cations) and carbocations have also been considered as reaction intermediates.^{1c,g,2} To judge the feasibilities of various pathways that have been proposed, ab initio molecular orbital calculations

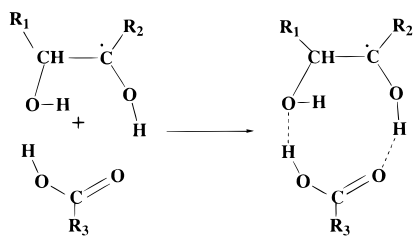
* To whom correspondence should be addressed.

[†] The Institute for Cancer Research.

[‡] University of Stockholm.

[§] Philadelphia University.

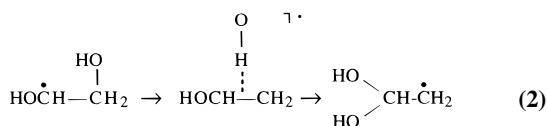
CHART 1



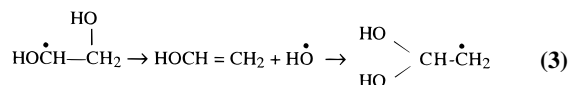
with full geometry optimization using the MP2(FC)/6-31G* level and single-point energy determinations at the MP2(FC)/6-311++G** level were carried out.³ In agreement with earlier MNDO SCF-MO calculations,⁴ the protonated 1,2-dihydroxyethyl-1-yl radical ($\text{H}_2\text{O}^+\text{CH}_2-\dot{\text{C}}\text{HOH}$) was found to be very unstable, breaking down spontaneously to give the vinyl alcohol radical cation ($\text{H}_2\text{C}-\dot{\text{C}}\text{HOH}^{\text{b}+}$) and water. H-atom transfer and H^+ dissociation then complete the dehydration process. In a similar reaction, protonation of the corresponding radical moiety ($\text{HOCH}(\text{R}_1)-\dot{\text{C}}(\text{R}_2)\text{OH}$) in the five-membered ring of a ribonucleotide by a thiol group, followed by the elimination of water, has been proposed in the reaction catalyzed by ribonucleotide reductase, in which ribonucleotide phosphates are converted to deoxyribonucleotide phosphates.^{5a,b}

A fundamentally different mechanism supported by density functional theory (DFT) calculations at the B3LYP/6-31+G* level has, however, been put forward recently to account for the elimination of water in the ribonucleotide reductase reaction and, by inference, in the diol dehydrase reaction.⁶ The key feature lies in the participation of a carboxylic acid group from an amino acid residue at the active site of the enzyme that interacts with a neutral (and not a protonated) radical. Two intermolecular hydrogen bonds are formed between the radical and the enzyme giving a nine-membered ring, see Chart 1. Bond rearrangement within this ring system brings about the transfer of the radical center from one carbon atom to the carbon atom adjacent to it. Subsequent elimination of H_2O occurs via the fission of the C–O bond at the new radical center.

To compare this “carboxylic acid cofactor” mechanism with other mechanisms that have been proposed for the dehydration of 1,2-dihydroxyethane, we have carried out similar DFT calculations on all the reacting species, utilizing formic acid as a model for the carboxylic acid at the active site. Geometries, ground-state electronic energies at 0 K, spin densities, atomic charges, vibrational frequencies, and total thermal energies and entropies at 298 K are reported for the separate reactant species (the 1,2-dihydroxyethyl-1-yl radical and formic acid) for the hydrogen-bonded reactant, for the transition state, for the hydrogen-bonded product, and for the separate product species (the formylmethyl radical, water, and formic acid). The changes in enthalpy, entropy, and free energy at 298 K have been calculated for each step, and the rate constant for the dehydration has been evaluated from the free energy of activation (hydrogen-bonded reactant \rightarrow transition state) to compare with the experimental value for the overall diol dehydration. Rate constants have also been evaluated from data in a previous paper for the mechanism in which an HO-bridge structure serves as a transition state in the formation of the 2,2-dihydroxyethyl-1-yl radical,^{2,3}



and for the mechanism in which fragmentation generates *syn*-vinyl alcohol and the HO radical, which then adds on to the other carbon atom, likewise giving the 2,2-dihydroxyethyl-1-yl radical,^{1h,j,k,7}



The formation of acetaldehyde and water is then accounted for either by H-atom transfer to the radical followed by H_2O fission from the resulting 2,2-dihydroxyethane, or by fission of H_2O from this radical followed by H-atom transfer to the resulting formylmethyl radical, $\text{O}=\text{CH}-\dot{\text{C}}\text{HO}_2^{\cdot}$.

Finally, a consideration of their molecular structures suggests that not only should the 1,2-diol radical be capable of forming a nine-membered hydrogen-bonded ring with formic acid but so also should the 1,2-diol. Further calculations have therefore been carried out to test this hypothesis, which implies that, in the dehydrase reaction, the diol substrate could already be locked onto binding groups at the active site *prior* to H-atom transfer to the 5'-deoxyadenosyl radical.^{1g}

Computational Methods

The calculations were carried out on computers at the Advanced Scientific Computing Laboratory, NCI-FCRF, using the GAUSSIAN 94 series of programs.⁸ Optimizations were performed with DFT using Becke's three parameter hybrid method where the nonlocal correlation functional is that of Lee, Yang, and Parr (B3LYP).^{9a-h} The 6-31+G* basis set was employed for all the structures, and in a few cases—the hydrogen-bonded reactant, the transition state, and the hydrogen-bonded product—the 6-311++G** basis set was used so as to explore the effect of using a more extended basis set on the structural parameters and reaction enthalpies.

Ground-state electronic energies at 0 K, E_e^0 , zero-point energies (zpe), total thermal energies at 298 K (θ), and entropies at 298 K (S^{298}) evaluated from vibrational frequencies calculated at the B3LYP/6-31+G*//B3LYP/6-31+G* level are listed in Table 1S of the Supporting Information. Atomic charges from natural population analyses (NPA),¹⁰ and spin densities were calculated at this level. The vibration frequencies were also used to determine whether the computed structures correspond to local minima or to saddle points (transition states) on the potential energy surface, PES.^{11a-c}

Single-point calculations using second-order Møller–Plesset (MP2) perturbation theory^{12a-d} with the more complete 6-311++G(2d,2p) basis set, and further calculations up to and including fourth-order using the 6-31++G** basis set were performed on all the structures involved in the dehydration and fragmentation processes. The electronic energies at 0 K at the MP2(FULL)/6-311++G(2d,2p)//B3LYP/6-31+G* level are also listed in Table 1S, and the energies at the MP4(SDTQ)-FC/6-31++G**//B3LYP/6-31+G* level and the MP4(SDTQ)-FC/6-31++G**//B3LYP/6-31++G** level in Table 2S. In addition, E_e^0 , θ , and S^{298} values from a previous paper,³ calculated at the MP2(FC)/6-311++G**//MP2(FC)/6-31G* level have been used to evaluate reaction enthalpies for dehydration via an HO-bridge structure as a transition state, and via the fragmentation process giving the HO radical and *syn*-vinyl alcohol, reactions 2 and 3 above.

The sum of E_e^0 and the total thermal energy θ at 298 K gives E^{298} , the total molecular energy at 298 K. Differences in E^{298} values for reactant and product species give the enthalpy

changes, ΔH^{298} , which, with the addition of a ΔnRT term where needed, would correspond to experimental gas-phase data.¹³ Likewise, differences between the calculated entropy values give the accompanying entropy changes, ΔS^{298} , and hence the free energy changes, using the equation $\Delta G^{298} = \Delta H^{298} - T\Delta S^{298}$. Basis set superposition error (BSSE) corrections have not been included in our results because they are very small at the computational levels we have employed, much smaller than the uncertainties inherent in the computational methods themselves.

In processes such as the ones studied here where charge separations might be present, it is important to account for possible polarizing effects of the protein. The dielectric effects from the surrounding protein were therefore obtained using the self-consistent isodensity polarized continuum model (SCI-PCM) and the B3LYP/6-31+G* computational level as implemented in the GAUSSIAN-94 program.^{8,14a,b} This is a simple model for treating long range solvent effects and considers the solvent as a macroscopic continuum with a dielectric constant ϵ . The solute is considered to fill a cavity in this continuous medium. The cavity is defined self-consistently in terms of a surface of constant charge density for the solute molecule. The default isodensity value of 0.0004 e/B³ was used, which has been found to yield volumes close to the observed molar volumes. The solvent effect is derived from the interactions of the surface potential with the dielectric continuum. The dielectric constant of the protein is the main empirical parameter of the model and it was chosen to be equal to 4, in line with previous suggestions for proteins.¹⁵ This value corresponds to a dielectric constant of about 3 for the protein itself and of 80 for the water medium surrounding the protein. This choice has recently been shown to give good agreement with experiment for two different electron-transfer processes in the bacterial photosynthetic reaction center.¹⁵

Estimation of Entropy Values for the Substrate and Reacting Species at the Active Site

We note at this point that the standard state to which these calculations pertain is the ideal gas at 1 atm pressure and 298.15 K, for which the molal volume V is 22 415 cm³. The value of S^{298} is made up of contributions from translation, rotation, vibration, and electronic entropy (applicable in the case of molecules in which there are one or more unpaired spins),

$$S^{298} = S_{\text{trans}}^{298} + S_{\text{rot}}^{298} + S_{\text{vib}}^{298} + S_{\text{elec}} \quad (4)$$

The contributions at the B3LYP/6-31+G**/B3LYP/6-31+G* and the MP2(FC)/6-31G**/MP2(FC)/6-31G* levels are listed in Tables 3S and 4S, respectively. S_{trans}^{298} , the major contribution, is evaluated using the Sackur–Tetrode equation, which reduces to $^{3/2}R \ln M + 25.8$, where M is the molecular weight.¹⁶ The parameter 25.8 includes as its major component the term $R \ln V$, which, V being 22 415 cm³, has a value of 19.9 cal/(mol K). A molal volume as large as this is clearly quite inappropriate for molecules reacting in the restricted environment at the active site. To calculate meaningful free energy changes, and hence compare the likelihood of alternative reaction pathways, it is therefore necessary to employ entropy values more in keeping with this restricted environment. The liquid state has been chosen as an appropriate model, instead of the solid, because the molecules are not static but retain some mobility.

In setting up an empirical equation for estimating entropies for the liquid state, S_{liq} , especially for species such as free radicals for which experimental values would be difficult if not

impossible to obtain, we have been guided by the success of empirical equations for the partial molal entropies of aqueous nonelectrolytes, which utilize the internal entropy, S_{int}^{298} , given by

$$S_{\text{int}}^{298} = S_{\text{rot}}^{298} + S_{\text{vib}}^{298} + S_{\text{elec}} \quad (5)$$

In one of these equations,¹⁷ it was assumed that S_{int}^{298} for the liquid state was the same as that for the gaseous state; in another,¹⁸ S_{int}^{298} was evaluated using the expression $(9.2N - S_s^0)$ where N is the number of “skeletal” bonded atoms minus hydrogens and S_s^0 are small structural correction terms. We have accordingly explored the validity of the simple empirical equation

$$S_{\text{liq}} = S_{\text{int}}^{298} + \phi \quad (6)$$

using the S^{298} and S_{liq} values for nonassociated liquids compiled by Stull, Westrum, and Sinke for 161 organic compounds.¹⁶ In each case S_{trans}^{298} was first calculated using the expression $^{3/2}R \ln M + 25.8$ and subtracted from S^{298} to give S_{int}^{298} . The value of ϕ was then obtained as the difference between S_{liq} and S_{int}^{298} . Grouping the data according to the number of “skeletal” bonded atoms, values of ϕ were obtained for $N = 3$ through 10. The mean values show little variation over the range $N = 3$ to $N = 8$, although with $N = 9$ and 10, for which there are fewer examples, there is a slight decrease.¹⁹ The mean value (taking all 161 examples into account) is 15.8, with a standard deviation of 1.8 cal/(mol K). S_{liq} values for all the molecules involved in this study, calculated using eq 6, are listed in the right-hand columns of Tables 3S and 4S and are later employed in the evaluation of ΔG^{298} for reactions occurring at the active site or in its immediate vicinity.

A further consequence of the restricted spatial environment at the active site is that a $P\Delta V$ (ΔnRT) term is no longer needed to correct ΔH^{298} for reactions in which there is a difference in the number of reactant and product species, since ΔV is far smaller than it is for the ideal gas state.

Results

Comparison with Experimental Values. Experimental data are available in only a few cases. With regard to geometrical parameters, the calculated bond lengths in formic acid, acetaldehyde, and water are consistently greater, by 0.007–0.010 Å, than those obtained spectroscopically.^{20–22} Nevertheless in formic acid the $r(\text{C—O})/r(\text{C=O})$ ratio, 1.115, compares very favorably with the r_e ratio of 1.116 obtained by microwave spectroscopy.²⁰ Likewise the $r(\text{C—H})/r(\text{O—H})$ ratios are very similar, 1.123 and 1.126, respectively. The OCO bond angle in formic acid is the same to within 0.3°, although the calculated values for the COH and HOH bond angles are greater by 1.2° and 1.6°, respectively.

As for the calculated and observed entropies, there is excellent agreement for water, 45.1₃ (calc) and 45.1₁ eu (obs), respectively, and close agreement for formic acid, 59.4 (calc) and 60.0 eu (obs).²³ The calculated and observed zero-point energies are also in excellent agreement for water, 13.2₃ and 13.2 kcal/mol respectively,²⁴ and there is close agreement between the values for formic acid, 21.1₄ and 20.3₄ kcal/mol, respectively.²⁵ The calculated enthalpy change for the dehydration process, reaction 1, -5.3 , -5.2 , and -5.5 kcal/mol at the B3LYP/6-31+G**//B3LYP/6-31+G*, MP2(FULL)/6-311++G(2d,2p)/B3LYP/6-31+G*, and MP2(FC)/6-311++G**//MP2(FC)/6-31G* levels,

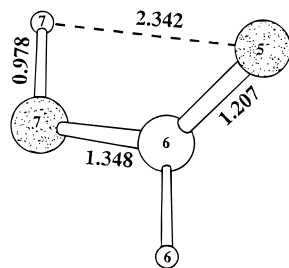


Figure 1. B3LYP/6-31+G* geometry-optimized structure of the cis conformer of formic acid (taking the H-atom of the H-O group and the O-atom of the C=O group as reference for the cis nomenclature). In this and all following figures oxygen atoms are stippled and hydrogen atoms are small.

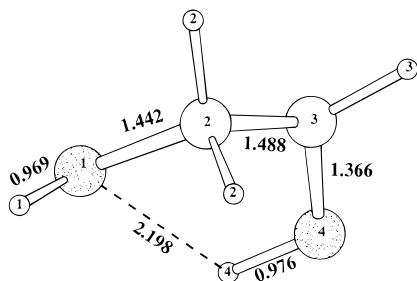


Figure 2. B3LYP/6-31+G* geometry-optimized structure of the cis conformer of the 1,2-dihydroxyeth-1-yl radical.

is in good agreement with the value of -4.9 ± 0.5 kcal/mol based on experimental heats of formation.²⁶

Structures of the Reacting Species. The molecular structures obtained with full geometry optimization at the B3LYP/6-31+G* computational level are depicted in Figure 1 for the (lower energy) cis conformer of formic acid,^{20,27a,b} in Figure 2 for the (lower energy) cis conformer of the 1,2-dihydroxyeth-1-yl radical, in Figure 3a-c for the reaction sequence (hydrogen-bonded reactant, transition state, and hydrogen-bonded product),

in Figure 4 for the formylmethyl radical, water, and acetaldehyde, in Figure 5 for the (lower energy) cis conformer of 1,2-dihydroxyethane,^{28a-c} and in Figure 6 for the hydrogen-bonded complex of 1,2-dihydroxyethane with formic acid. For convenience, to keep consistent numbering throughout the reaction sequence, the two oxygen atoms of 1,2-dihydroxyethane and its derivatives are labeled O₍₁₎ and O₍₄₎ and the carbon atoms C₍₂₎ and C₍₃₎. Formic acid is labeled with O₍₅₎, O₍₇₎, and C₍₆₎.

1,2-Dihydroxyeth-1-yl Radical. A cis and a trans conformer of the 1,2-dihydroxyeth-1-yl radical have been identified. They are similar to those for the parent 1,2-dihydroxyethane.^{28a-c} The cis conformer (see Figure 2) is lower in energy compared to the trans isomer by 2.3 kcal/mol, calculated from the E^{298} values at the B3LYP/6-31+G*/B3LYP/6-31+G* and MP2(FULL)/6-311++G(2d,2p)/B3LYP/6-31+G* levels (+2.3₃ and +2.3₁ kcal/mol, respectively). This cis conformer has been used in the evaluation of the enthalpy change for the formation of the hydrogen-bonded reactant.

Hydrogen-Bonded Reactant. An examination of molecular models shows that the presence of the four-membered ring in the cis conformer of formic acid and the five-membered ring in the cis conformer of the 1,2-dihydroxyeth-1-yl radical facilitates the formation of the nine-membered ring. With these lower energy conformers approaching each other, as shown in Figure 7, all that is required is a changeover from the *intramolecular* hydrogen-bonding interactions, O₍₁₎-H₍₄₎ and O₍₅₎-H₍₇₎, to the *intermolecular* hydrogen-bonding interactions O₍₁₎-H₍₇₎ and O₍₅₎-H₍₄₎. No major reorientation such as internal rotation is necessary.

The Transition State. The transition state for the elimination of water has been identified, see Figure 3b. Notable changes in interatomic distances upon its formation from the hydrogen-bonded reactant are (i) an increase in O₍₁₎-C₍₂₎ from 1.480 to 1.908 Å, a decrease in O₍₁₎-H₍₇₎ from 1.674 to 1.114 Å, and an increase in O₍₇₎-H₍₇₎ from 1.008 to 1.344 Å, indicating that already there is partial separation of a somewhat distorted

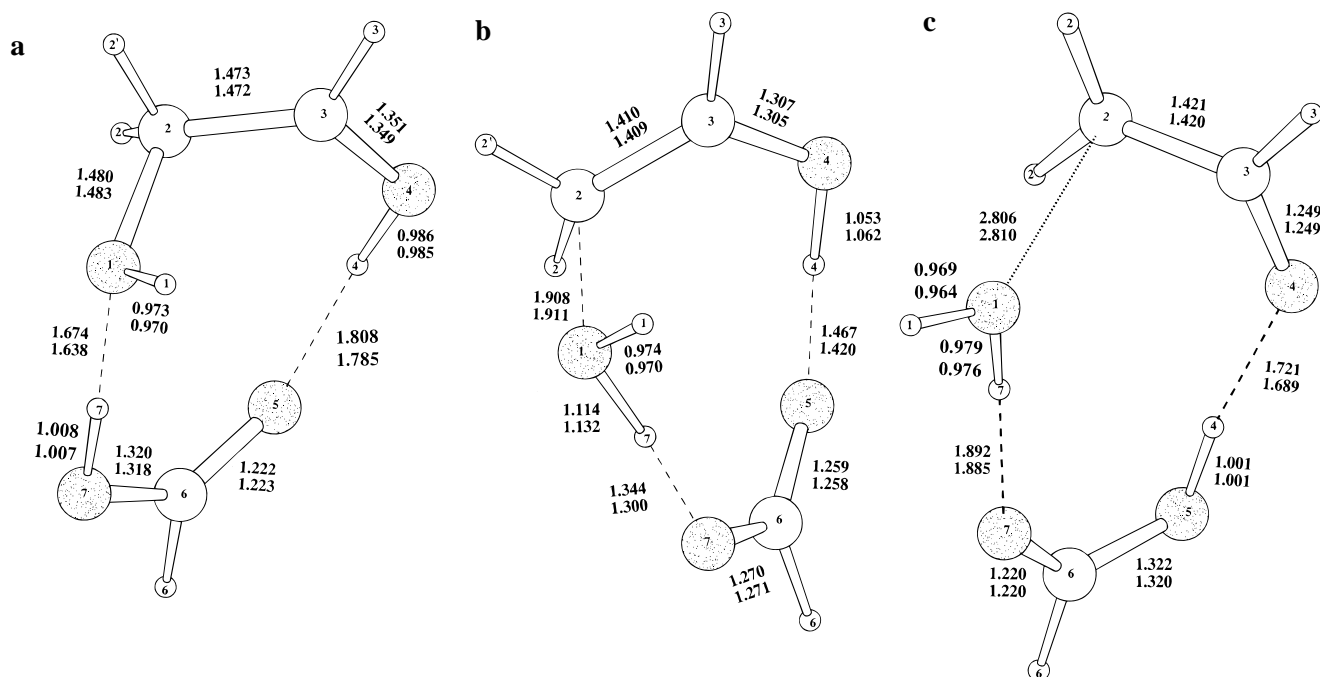


Figure 3. (a) Geometry-optimized structure of the hydrogen-bonded reactant using the B3LYP/6-31+G* (upper values) and the B3LYP/6-31++G** (lower values) computational levels. Geometry-optimized structure of the transition state using the B3LYP/6-31+G* (upper values) and the B3LYP/6-31++G** (lower values) computational levels. (c) Geometry-optimized structure of the hydrogen-bonded product using the B3LYP/6-31+G* (upper values) and the B3LYP/6-31++G** (lower values) computational levels.

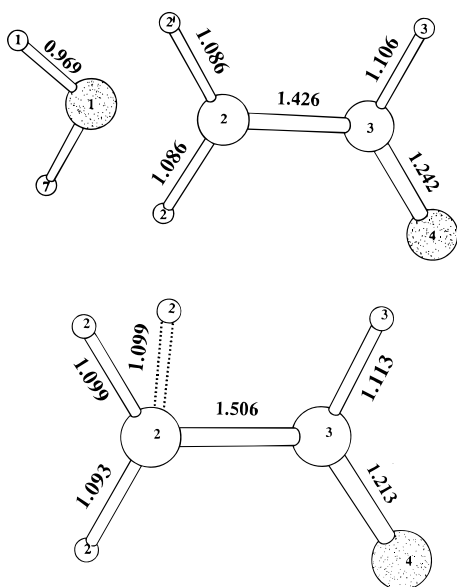


Figure 4. B3LYP/6-31+G* geometry-optimized structures of the formylmethyl radical, water, and acetaldehyde.

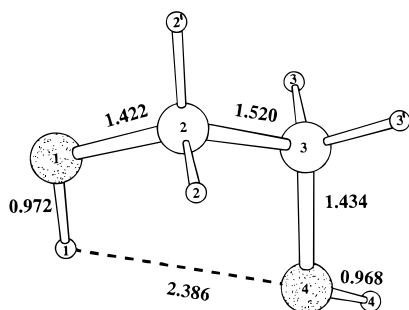


Figure 5. B3LYP/6-31+G* geometry-optimized structure of the cis conformer of 1,2-dihydroxyethane.

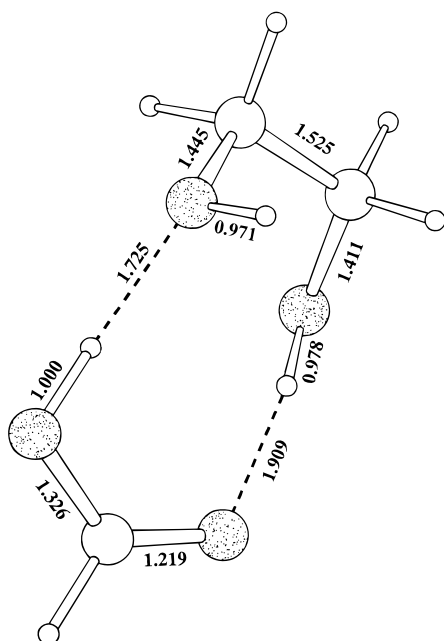
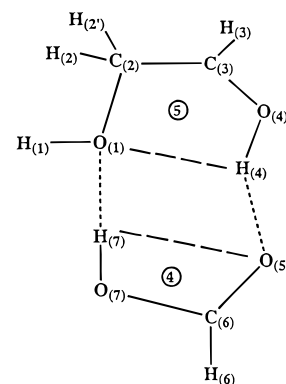


Figure 6. B3LYP/6-31+G* geometry-optimized structure of the nine-membered hydrogen-bonded ring formed between formic acid and 1,2-dihydroxyethane.

water molecule, $H_{(1)}O_{(1)}H_{(7)}$; (ii) a decrease in $O_{(7)} - -C_{(6)}$ from 1.320 to 1.270 Å, together with an increase in $O_{(5)} - -C_{(6)}$ from 1.222 to 1.259 Å, in accord with the partial conversion of HO-



Nine-membered ring

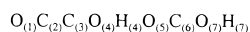


Figure 7. Schematic diagram illustrating the approach of the cis conformer of formic acid (lower four-membered ring) up to the cis conformer of the 1,2-dihydroxyethyl-1-yl radical (upper five-membered ring) to give the hydrogen-bonded reactant. The dashed lines depict the intramolecular hydrogen-bonding interactions in the separate molecules, and the dotted lines the intermolecular hydrogen-bonding in the nine-membered ring.

C into $O=C$ bonding in the formic acid moiety, and; (iii) a decrease in $C_{(3)} - -O_{(4)}$ from 1.351 to 1.307 Å, indicating partial double bond formation (in keeping with the eventual formation of the formylmethyl radical).

In the intermolecular hydrogen-bonding system the angles $O_{(1)} \cdots H_{(7)} \cdots O_{(7)}$ and $O_{(4)} \cdots H_{(4)} \cdots O_{(5)}$ remain close to 180° , i.e., 171.6° and 173.5° , respectively; see Table 1A. In the hydrogen-bonded reactant (Figure 3a) $O_{(7)}$ is the oxygen atom of the donor HO group with $O_{(1)}$ the oxygen atom of the acceptor $O=C$ group, and $O_{(4)}$ is the oxygen atom of the donor HO group with $O_{(5)}$ the oxygen atom of the acceptor $O=C$ group. These relationships are reversed in the hydrogen-bonded product; see Chart 2 and Table 1B.

Since the transition state involves the transfer of hydrogens, there is a possibility that the tunneling effect could result in a significant increase in the transmission coefficient, and hence the rate constant. This increase has been estimated using Wigner's transmission coefficient $\kappa^w(T)$, given by the expression

$$\kappa^w(T) = 1 + \frac{1}{24} \left(\frac{\hbar \omega^\ddagger}{RT} \right)^2 \quad (7)$$

where ω^\ddagger is the imaginary frequency of the unbound normal mode at the saddle point.²⁹ From the vibration frequency analysis ω^\ddagger is found to have a value a little less than -400 cm^{-1} , which, upon substitution in the above expression, gives $\kappa^w(298) = 1.16$. The reaction would thus go only 1.16 times faster with the correction than without, not a highly significant increase.

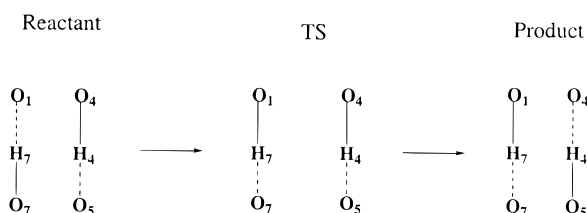
Hydrogen-Bonded Product. Proceeding along the same reaction pathway, the hydrogen-bonded product has been identified; see Figure 3c. The structure is entirely in keeping with the incipient formation of the formylmethyl radical, water, and formic acid, prior to their eventual separation.

Extent of the Reaction in the Transition State. The changes in the interatomic distances between the carbon and oxygen atoms in going from the hydrogen-bonded reactant to the hydrogen-bonded product via the transition state are listed in Table 2. All but the $C \cdots C$ distance, which passes through a minimum value in the transition state, either increase, i.e., $O_{(1)} - -C_{(2)}$ and $O_{(5)} - -C_{(6)}$, or decrease, i.e., $C_{(3)} - -O_{(4)}$ and $C_{(6)} - -O_{(7)}$. The average increase in the transition state amounts

TABLE 1: (A) Intermolecular Hydrogen Bridge Angles, $\angle O_{(1)}\cdots H_{(7)}\cdots O_{(7)}$ and $\angle O_{(4)}\cdots H_{(4)}\cdots O_{(5)}$, in deg, and (B) Intermolecular Distances, $O_{(1)}\cdots H_{(7)}$, $H_{(7)}\cdots O_{(7)}$, $O_{(4)}\cdots H_{(4)}$, and $H_{(4)}\cdots O_{(5)}$, in Å, in the Hydrogen-Bonded Reactant, the Transition State, and the Hydrogen-Bonded Product (See Chart 2 and Figures 3a–c)^a

molecule	A		B			
	$\angle O_{(1)}\cdots H_{(7)}\cdots O_{(7)}$	$\angle O_{(4)}\cdots H_{(4)}\cdots O_{(5)}$	$O_{(1)}\cdots H_{(7)}$	$H_{(7)}\cdots O_{(7)}$	$O_{(4)}\cdots H_{(4)}$	$H_{(4)}\cdots O_{(5)}$
hydrogen-bonded reactant	178.0	176.1	1.674	1.008	0.986	1.808
transition state	(177.4)	(176.0)	(1.638)	(1.007)	(0.985)	(1.785)
	175.6	176.9	1.114	1.344	1.053	1.467
hydrogen-bonded product	(175.1)	(175.7)	(1.132)	(1.300)	(1.062)	(1.420)
	173.5	171.6	0.979	1.892	1.721	1.001
	(173.2)	(171.3)	(0.976)	(1.885)	(1.689)	(1.001)

^a The values in parentheses refer to the geometry optimization using the B3LYP/6-31++G** computational level.

CHART 2**TABLE 2: Interatomic Distances, in Å, between the Carbon and Oxygen Atoms in the Hydrogen-Bonded Reactant, the Transition State, and the Hydrogen-Bonded Product and the Percentage Change in Going from the Reactant to the Transition State^a**

interatomic distance	H-bonded reactant	TS	H-bonded product	percentage change
$O_{(1)}-C_{(2)}$	1.480 (1.483)	1.908 (1.911)	2.806 (2.810)	32 (32)
$C_{(2)}-C_{(3)}$	1.473 (1.472)	1.410 (1.409)	1.421 (1.420)	
$C_{(3)}-O_{(4)}$	1.351 (1.349)	1.307 (1.305)	1.249 (1.249)	43 (44)
$O_{(5)}-C_{(6)}$	1.222 (1.223)	1.259 (1.258)	1.322 (1.320)	37 (36)
$C_{(6)}-O_{(7)}$	1.320 (1.318)	1.270 (1.271)	1.220 (1.220)	50 (48)

^a The values in parentheses refer to the geometry optimization using the B3LYP/6-31++G** computational level.

to 35% of the overall change, and the average decrease to 47%, no matter whether the B3LYP/6-31+G* or B3LYP/6-31++G** data are used.

Hydrogen-Bonding Characteristics. The hydrogen-bridge angles $\angle O_{(1)}\cdots H_{(7)}\cdots O_{(7)}$ and $\angle O_{(4)}\cdots H_{(4)}\cdots O_{(5)}$ are all quite close to the 180° value for optimal hydrogen bonding,³⁰ even though the nine-membered ring is nonplanar.³¹ These values are little affected by the use of the more extended B3LYP/6-31++G** method (see Table 2A), even though, of all the geometrical parameters, the $O_{(1)}\cdots H_{(7)}$ and $H_{(4)}\cdots O_{(5)}$ distances are most affected by the choice of basis set, shortening by up to 0.047 Å (compare Table 1B and Table 2).

Hydrogen-Bonding between *cis*-1,2-Dihydroxyethane and Formic Acid. The formation of a nine-membered ring with two intermolecular hydrogen bonds joining the diol and formic acid, like that formed by the diol radical, has been substantiated. Hence, in the dehydrase reaction, the diol substrate could already be locked onto a binding carboxylic acid group at the active site prior to H-atom transfer to the 5'-deoxyadenosyl radical. The structure is shown in Figure 6. Using the same notation as in Figures 3 and 7, the hydrogen-bridge angles $\angle O_{(1)}\cdots H_{(7)}\cdots O_{(7)}$ and $\angle O_{(4)}\cdots H_{(4)}\cdots O_{(5)}$ are 172.1° and 170.1°, respectively, a few degrees smaller than the values for the diol radical–formic acid structure. The absence of the radical grouping –CHOH in the diol precludes the facile dehydration via the transition state shown in Figure 3b. Nevertheless, the search for a different kind of transition state did locate such a structure. In essence, the formic acid component is much more distant from the diol than in the diol radical TS, and there is an interchange in the position

of the C=O and C–OH bonds. A water molecule is in the process of being formed by combination of an H-atom and an HO-group from the *same* carbon atom in the diol, which, in turn, is partly converted into a substituted carbene structure in which one of the H-atoms in the carbene (CH₂) is replaced by the HOCH₂ group, giving as the overall reaction



For such an unlikely reaction it is not surprising to find a very high energy barrier of 76 kcal/mol.

Distortion Geometry. The changes in bond lengths and angles in the formation of the nine-membered ring structures from the separate molecules—the diol radical plus formic acid and the diol plus formic acid—are listed in Table 3A,B. With only one exception, the $C_{(2)}\text{--}C_{(3)}$ bond length, all the other changes show that ring formation brings about a very similar distortion of the geometries of the separate molecules. The increases in bond angle which accompany ring formation are most striking, exceeding 5° in several instances and are in large part responsible for an increase in the $O_{(1)}\cdots H_{(4)}$ distance in the radical from 2.198 to 2.929 Å, and an increase in the $H_{(7)}\cdots O_{(5)}$ distance in the formic acid from 2.342 to 2.410 Å. With regard to the formation of the intermolecular hydrogen bonds, the increase in the length of both the donor groups, $O_{(7)}\text{--}H_{(7)}$ and $O_{(4)}\text{--}H_{(4)}$, and the acceptor groups, $O_{(1)}\text{--}C_{(2)}$ and $O_{(5)}\text{--}C_{(6)}$, is in keeping with that found for the intramolecular hydrogen-bonding interaction present in four-, five-, and six-membered ring systems.^{32a–c}

Origin of the Hydrogen Atoms in the Water Molecule. In mechanisms in which the water is formed by dehydration of a 1,1-diol intermediate produced by the interchange of a hydrogen atom and a hydroxyl group on adjacent carbon atoms in the 1,2-diol, both hydrogen atoms come from the same diol molecule,^{1b,c,f}



By contrast, it is found that in the catalytic cycle with formic acid as cofactor, these hydrogen atoms originate in different molecules. In the first reaction cycle, one water hydrogen atom comes from the HO group of the original formic acid ($O_{(7)}$), and the other hydrogen atom from the HO group in the CH₂–OH grouping in the diol radical ($O_{(1)}$), as shown in Figure 7. The formic acid is regenerated: $H_{(4)}$ from the CHOH grouping in the diol radical is transferred to $O_{(5)}$, giving the HO group, and $O_{(7)}$ becomes the carbonyl oxygen. In the second cycle, one hydrogen atom comes from the HO group in this regenerated formic acid, and the other hydrogen atom from the HO group in the CH₂OH grouping in a newly bound diol radical, and likewise for subsequent cycles.

Electronic Properties. Spin Density Changes in the Course of the Catalytic Reaction. As expected, the spin density is

TABLE 3: Changes in the Bond Lengths and Bond Angles in the Formation of the Nine-Membered Ring Structures from the Separate Molecules: (A) 1,2-Dihydroxyeth-1-yl Radical plus Formic Acid; (B) 1,2-Dihydroxyethane plus Formic Acid

parameter/molecule	molecule		
	separate molecule	in large ring	difference
A. 1,2-Dihydroxyeth-1-yl Radical plus Formic Acid			
1. bond lengths ^a			
a. <i>cis</i> -1,2-dihydroxyeth-1-yl radical			
O ₍₁₎ -C ₍₂₎	1.442	1.480	+0.038
C ₍₂₎ -C ₍₃₎	1.488	1.473	-0.015
C ₍₃₎ -O ₍₄₎	1.366	1.351	-0.015
O ₍₄₎ -H ₍₄₎	0.976	0.986	+0.010
b. formic acid			
O ₍₅₎ -C ₍₆₎	1.207	1.222	+0.015
O ₍₆₎ -O ₍₇₎	1.348	1.320	-0.028
O ₍₇₎ -H ₍₇₎	0.978	1.008	+0.030
2. bond angles ^b			
a. <i>cis</i> -1,2-dihydroxyeth-1-yl radical			
O ₍₁₎ C ₍₂₎ C ₍₃₎	106.8	113.8	+7.0
O ₍₂₎ C ₍₃₎ O ₍₄₎	117.4	122.5	+5.1
C ₍₃₎ O ₍₄₎ H ₍₄₎	106.9	111.9	+5.0
b. formic acid			
O ₍₅₎ C ₍₆₎ O ₍₇₎	125.1	126.4	+1.3
C ₍₆₎ O ₍₇₎ H ₍₇₎	107.8	111.2	+3.4
B. 1,2-Dihydroxyethane plus Formic Acid			
1. bond lengths ^a			
a. <i>cis</i> -1,2-dihydroxyethane			
O ₍₁₎ -C ₍₂₎	1.434	1.445	+0.011
C ₍₂₎ -C ₍₃₎	1.520	1.525	+0.005
C ₍₃₎ -O ₍₄₎	1.422	1.411	-0.011
O ₍₄₎ -H ₍₄₎	0.972	0.978	+0.006
b. formic acid			
O ₍₅₎ -C ₍₆₎	1.207	1.219	+0.012
C ₍₆₎ -O ₍₇₎	1.348	1.326	-0.022
O ₍₇₎ -H ₍₇₎	0.978	1.000	+0.022
2. bond angles ^b			
a. <i>cis</i> -1,2-dihydroxyethane			
O ₍₁₎ C ₍₂₎ O ₍₃₎	106.5	113.2	+6.7
C ₍₂₎ C ₍₃₎ O ₍₄₎	111.9	113.7	+1.8
C ₍₃₎ O ₍₄₎ H ₍₄₎	106.9	110.3	+3.4
b. formic acid			
O ₍₅₎ C ₍₆₎ O ₍₇₎	125.1	126.1	+1.0
O ₍₆₎ O ₍₇₎ H ₍₇₎	107.8	110.5	+2.7

^a In Å. ^b In deg.**TABLE 4: Total Atomic Spin Densities in the O₍₁₎-C₍₂₎-C₍₃₎-O₍₄₎ Chain Calculated from Population Analyses Using the B3LYP/6-31+G* SCF Densities**

species	O ₍₁₎	C ₍₂₎	C ₍₃₎	O ₍₄₎	total
dihydroxyethyl radical	-0.012	-0.030	+0.909	+0.111	0.978
H-bonded reactant	-0.004	+0.011	+0.856	+0.139	1.002
transition state	+0.167	+0.251	+0.419	+0.196	1.033
H-bonded product	+0.006	+0.858	-0.086	+0.303	1.081
formylmethyl radical		+0.888	-0.158	+0.352	1.082

primarily located on C₍₃₎ in the isolated dihydroxyeth-1-yl radical HOCH₂-CHOH and in the hydrogen-bonded reactant (Figures 2 and 3a), and on C₍₂₎ in the formylmethyl radical H₂C-CHO and the hydrogen-bonded product (Figures 4 and 3c); see Table 4. Next in importance, there is significant spin density on O₍₄₎, increasing from 0.111 to 0.352 in the course of the reaction. In the transition state the density is spread over all four atoms: O₍₁₎ 16%, C₍₂₎ 24%, C₍₃₎ 41% and O₍₄₎ 19%.

Changes in the NPA Charges on the Various Atoms Brought about by the Formation of the Nine-Membered Ring. The charges and the alterations in charge that accompany the formation of the hydrogen-bonded ring structures are listed in Table 5A,B for the 1,2-dihydroxyethyl radical and formic acid, and for 1,2-dihydroxyethane and formic acid, respectively. For

TABLE 5: Changes in the Natural Charge on the Various Atoms Brought about by the Formation of the Nine-Membered Ring: (A) *cis*-1,2-Dihydroxyeth-1-yl Radical plus Formic Acid; (B) *cis*-1,2-Dihydroxyethane plus Formic Acid^a

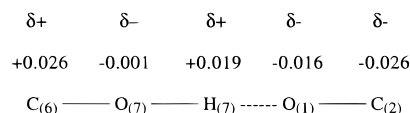
atom	separate components	ring system	difference, δ ^b
A. <i>cis</i> -1,2-Dihydroxyeth-1-yl Radical plus Formic Acid			
O ₍₁₎	-0.795	-0.811	-0.016
C ₍₂₎	-0.209	-0.235	-0.026
C ₍₃₎	+0.087	+0.069	-0.018
O ₍₄₎	-0.719	-0.706	+0.013
H ₍₄₎	+0.518	+0.530	+0.012
O ₍₅₎	-0.594	-0.664	-0.070
C ₍₆₎	+0.641	+0.667	+0.026
O ₍₇₎	-0.719	-0.720	-0.001
H ₍₇₎	+0.512	+0.531	+0.019
∑H(C) ^c	+0.780	+0.833	+0.053
H ₍₁₎	+0.499	+0.505	+0.006
B. <i>cis</i> -1,2-Dihydroxyethane plus Formic Acid			
O ₍₁₎	-0.796	-0.801	-0.005
C ₍₂₎	-0.146	-0.145	+0.001
C ₍₃₎	-0.135	-0.141	-0.006
O ₍₄₎	-0.780	-0.793	-0.013
H ₍₄₎	+0.503	+0.517	+0.014
O ₍₅₎	-0.594	-0.649	-0.055
C ₍₆₎	+0.641	+0.659	+0.018
O ₍₇₎	-0.719	-0.723	-0.004
H ₍₇₎	+0.512	+0.531	+0.019
∑H(C) ^c	+1.014	+1.038	+0.024
H ₍₁₎	+0.501	+0.509	+0.008

^a For the numbering system see Figures 3a and 7. ^b A positive value for δ indicates that the atom concerned has become more positive, i.e., has lost electronic charge; a negative value indicates that the atom concerned has become more negative, i.e., has gained electronic charge.

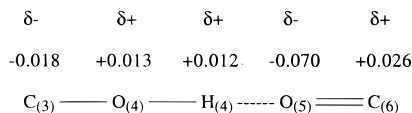
^c The sum of the charges on the hydrogen atoms bonded to carbon.

each of the nine atoms that make up the large ring, with the sole exception of C₍₂₎, the sign of the change in charge, i.e., whether there is a loss or a gain of electronic charge, is the same in both cases.

A distinction can be made between the two types of hydrogen bonding depending on whether the acceptor atom is the O-atom of a hydroxyl group or a carbonyl group. When it is the O-atom of the hydroxyl group in C₍₆₎O₍₇₎H₍₇₎, the sequence of electronic loss (δ+) or gain (δ-) on forming the nine-membered ring is



whereas when it is the O-atom of the carbonyl group C₍₆₎O₍₅₎, the sequence is



The two types of hydrogen-bonding have in common a loss of charge on the bridging H-atom (H₍₇₎ and H₍₄₎) together with a gain of charge on the acceptor O-atom (O₍₁₎ and O₍₅₎). Otherwise, there are significant differences.

The greatest change in charge occurs on O₍₅₎, i.e., -0.070 and -0.055; see Table 5A,B. From a summation of the individual charges on the component molecules, it appears that this change on O₍₅₎ is largely responsible for an overall transfer of charge from the diol radical, and from the diol, to the formic

TABLE 6: Changes in the Electronic Energy at 0 K, ΔE_e^0 , Calculated Using the MP4(SDTQ)(FC)/6-31++G Computational Level for the Following Steps in the Formic Acid Catalyzed Dehydration of the 1,2-Dihydroxyeth-1-yl Radical: (i) Hydrogen-Bonded Reactant \rightarrow Transition State, (ii) Hydrogen-Bonded Product \rightarrow Transition State, (iii) Hydrogen-Bonded Reactant \rightarrow Hydrogen-Bonded Product^a**

energy calculation	B3LYP/6-31+G* geom			B3LYP/6-31++G** geom		
	ΔE_e^0 (i)	ΔE_e^0 (ii)	ΔE_e^0 (iii)	ΔE_e^0 (i)	E_e^0 (ii)	E_e^0 (iii)
UMP2	16.2	14.7	+1.5	16.0	14.6	+1.4
PMP2	15.9	19.6	-3.7	15.7	19.4	-3.7
UMP3	21.7	22.1	-0.4	21.6	22.0	-0.4
PMP3	21.7	25.7	-4.0	21.5	25.6	-4.1
UMP4(DQ)	22.0	22.9	-0.9	21.9	23.0	-1.1
UMP4(SDQ)	19.7	21.3	-1.6	19.6	21.3	-1.7
UMP4(SDTQ)	17.0	17.7	-0.7	16.8	17.6	-0.8

^a Using structures geometry-optimized at the B3LYP/6-31+G* and B3LYP/6-31++G** computational levels.

acid, amounting to 0.024 and 0.025, respectively, upon formation of the nine-membered rings.

Thermodynamic Data. Values for the reaction parameters ΔE_e^0 , ΔH^{298} , ΔS^{298} , and ΔG^{298} , obtained using two levels for geometry optimization, more extended basis sets, and the inclusion of electron correlation ranging from MP2 to MP4-(SDTQ), are listed in Tables 6 and 7, and in Tables 3S and 4S of the Supporting Information.

The values of ΔE_e^0 in Table 6 show that the use of the more extended basis set in the geometry optimization, using the B3LYP/6-31++G** level instead of the B3LYP/6-31+G* level, has remarkably little effect. This might have been expected in view of the almost identical increments in the C–O and C–C bond distances in going from the hydrogen-bonded reactant to the transition state and from the transition state to the hydrogen-bonded product (see Table 2) and in view of the very similar hydrogen-bridge angles, $\angle O_{(1)} - -H_{(7)} - -O_{(7)}$ and $\angle O_{(4)} - -$

$H_{(4)} - -O_{(5)}$ (see Table 1A). Nevertheless, it is rather surprising since several of the H–O distances show a significant decrease with the B3LYP/6-31++G** optimization, indicating a tightening of the nine-membered ring structures: notably, $O_{(1)} - -H_{(7)}$ in the reactant, $H_{(7)} - -O_{(7)}$ in the transition state, $O_{(4)} - -H_{(4)}$ in the product, and $H_{(4)} - -O_{(5)}$ in both the reactant and in the transition state, are shorter by as much as 0.036, 0.044, 0.032, 0.023, and 0.047 Å, respectively; see Table 1B.

The values for ΔH^{298} in Table 7 show the combined effect of basis set extension and the inclusion of electron correlation on ΔH^{298} for the various steps and for the overall dehydration of the 1,2-dihydroxyethyl radical. There is a general tendency for the values to become less exothermic (or more endothermic) at the higher levels. For the interchange of the hydrogen-bonding and intramolecular electron transfer in the nine-membered rings in going from the hydrogen-bonded reactant to the transition state, and from the transition state to the hydrogen-bonded product, the values suggest that any further inclusion of electron correlation beyond the MP4(SDTQ) level would make no significant difference.

We note in passing that the difference between the thermal energies of the reactant and product species can make a significant contribution to ΔH^{298} . For example, in the first, second, and sixth reactions in Table 7 the contributions are +2.2, -3.7, and 4.1 kcal/mol, respectively.

For the reactions at the active site in which there is a difference in the number of reactant and product species, namely the first, fourth, and sixth in Table 7, the modified S^{298} values and, to a lesser extent, the absence of the ΔnRT terms result in very substantial changes in ΔG^{298} . Compared with the gas-phase ΔS^{298} values the increments, $\delta\Delta S^{298}$, are +20.0, -37.7, and -17.7 cal/(mol K), respectively, resulting in ΔG^{298} increments of -6.0, +11.2, and +5.3 kcal/mol. The absence of the ΔnRT terms change ΔG^{298} by +0.6, -1.2, and -0.6 kcal/mol, respectively.

TABLE 7: ΔH^{298} , ΔS^{298} , and ΔG^{298} for the Reaction Steps in the Gas Phase, and at the Active Site, for the Formic Acid Catalyzed Dehydration of the 1,2-Dihydroxyeth-1-yl Radical, with E_e^0 Values (Going from Top to Bottom) Calculated Using the B3LYP/6-31+G*, the MP2(FULL)/6-311++G(2d,2p), the MP2(FC)/6-31++G, and the MP4(SDTQ)FC/6-31++G** Methods: B3LYP/6-31+G* Geometry Optimization^a**

reaction	ideal gas			active site		
	ΔH^{298}	ΔS^{298}	ΔG^{298}	ΔH^{298}	ΔS^{298}	ΔG^{298}
<i>cis</i> -1,2-dihydroxyeth-1-yl radical + formic acid \rightarrow hydrogen-bonded reactant	-14.5	-35.7	-3.9	-13.9	-15.7	-9.3
	-14.4	-35.7	-3.8	-13.8	-15.7	-9.1
	-14.3	-35.7	-3.7	-13.7	-15.7	-9.0
	-10.5	-35.7	+0.2	-9.9	-15.7	-5.2
hydrogen-bonded reactant \rightarrow TS	+8.8	-4.9	+10.3	+8.8	-4.9	+10.3
	+12.4	-4.9	+13.9	+12.4	-4.9	+13.9
	+12.2	-4.9	+13.7	+12.2	-4.9	+13.7
	+13.3	-4.9	+14.7	+13.3	-4.9	+14.7
TS \rightarrow hydrogen-bonded product	-13.0	+17.6	-18.3	-13.0	+17.6	-18.3
	-17.2	+17.6	-22.4	-17.2	+17.6	-22.4
	-17.6	+17.6	-22.8	-17.6	+17.6	-22.8
	-15.7	+17.6	-20.9	-15.7	+17.6	-20.9
hydrogen-bonded product \rightarrow formylmethyl radical + formic acid + H ₂ O	+12.9	+58.9	-4.6	+11.7	+21.2	+5.4
	+14.8	+58.9	-2.8	+13.6	+21.2	+7.3
	+15.0	+58.9	-2.5	+13.8	+21.2	+7.5
	+12.5	+58.9	-5.1	+11.3	+21.2	+4.8
hydrogen-bonded reactant \rightarrow hydrogen-bonded product	-4.2	+12.7	-8.0	-4.2	+12.7	-8.0
	-4.8	+12.7	-8.6	-4.8	+12.7	-8.6
	-5.4	+12.7	-9.2	-5.4	+12.7	-9.2
	-2.5	+12.7	-6.2	-2.5	+12.7	-6.2
<i>cis</i> -1,2-dihydroxyeth-1-yl radical \rightarrow formylmethyl radical + H ₂ O	-5.8	+35.9	-16.5	-6.4	+18.2	-11.8
	-4.4	+35.9	-15.1	-5.0	+18.2	-10.4
	-4.7	+35.9	-15.4	-5.3	+18.2	-10.7
	-0.5	+35.9	-11.2	-1.1	+18.2	-6.5

^a Values of θ from Table 1S and S^{298} from Table 3S (Supporting Information). For the second step the values are the enthalpy, the entropy, and the free energy of activation.

TABLE 8: ΔH^{298} , ΔS^{298} , and ΔG^{298} for the Reaction Steps in the Gas Phase, and at the Active Site, for the Dehydration of the 1,2-Dihydroxyeth-1-yl Radical via an HO-Bridge Structure (Transition State), Reaction 2, and via a Fragmentation Process Involving Formation of the HO Radical and *syn*-Vinyl Alcohol, Reaction 3, Calculated at the MP2(FC)/6-311++G**//MP2(FC)/6-31+G* Level and (in parentheses) at the MP4(SDTQ)FC/6-31++G**//B3LYP/6-31+G* Level: S^{298} data from Table 4S (Supporting Information)

reaction	ideal gas			active site		
	ΔH^{298}	ΔS^{298}	ΔG^{298}	ΔH^{298}	ΔS^{298}	ΔG^{298}
<i>cis</i> -1,2-dihydroxyeth-1-yl radical \rightarrow H–O bridge intermediate (transition state)	–28.6	+8.7	+26.0	+28.6	+8.7	+26.0
H–O bridge intermediate \rightarrow 2,2-dihydroxyeth-1-yl radical	–32.8	–9.8	–29.9	–32.8	–9.8	–29.9
<i>cis</i> -1,2-dihydroxyeth-1-yl radical \rightarrow HO radical + <i>syn</i> -vinyl alcohol	+27.7	+31.5	+18.3	+27.1	+13.8	+23.0
			(+17.2)			(+21.8)
HO radical + <i>syn</i> -vinyl alcohol \rightarrow 2,2-dihydroxyeth-1-yl radical	–32.0	–32.6	–22.3	–31.4	–14.9	–26.9
2,2-dihydroxyeth-1-yl radical \rightarrow H ₂ O + formylmethyl radical	–2.8	+36.2	–13.6	–3.4	+18.4	–8.9
<i>cis</i> -1,2-dihydroxyeth-1-yl radical \rightarrow 2,2-dihydroxyeth-1-yl radical	–4.2	–1.1	–3.9	–4.2	–1.1	–3.9
<i>cis</i> -1,2-dihydroxyeth-1-yl radical \rightarrow H ₂ O + formylmethyl radical	–7.0	+35.1	–17.5	–7.6	+17.3	–12.8
			(–11.2)			(–6.5)

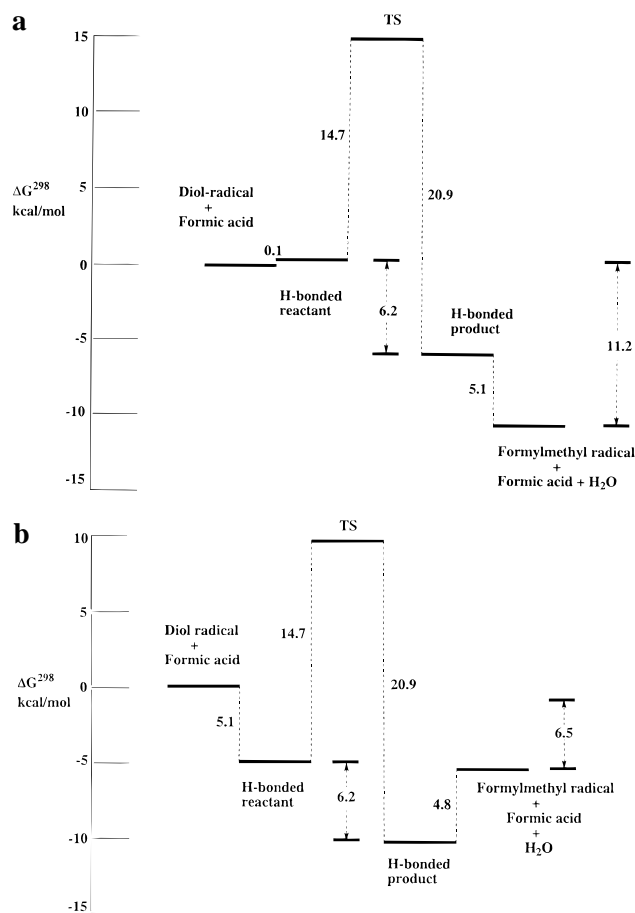


Figure 8. (a) Free energy increments, in kcal/mol, for the successive steps in the formic acid-catalyzed dehydration of the *cis*-1,2-dihydroxyeth-1-yl radical in the gas phase taking the diol radical and formic acid as zero, calculated at the MP4(SDTQ)FC/6-31++G**//B3LYP/6-31+G* level. (b) Free energy increments, in kcal/mol, for the successive steps in the formic acid-catalyzed dehydration of the *cis*-1,2-dihydroxyeth-1-yl radical at the active site of the enzyme taking the diol radical and formic acid as zero, calculated at the MP4(SDTQ)FC/6-31++G**//B3LYP/6-31+G* level.

The changes in free energy at the various stages of the dehydration process are depicted in Figure 8a,b for the gas phase and for the more restricted environment of the active site, respectively. For the catalysis itself the relevant species are the hydrogen-bonded reactant, the transition state, and the hydrogen-bonded product. Reaction of the next diol radical with the hydrogen-bonded product, regenerating the hydrogen-bonded reactant, would entail only a transfer of hydrogen-bonding from

one structure to another and, since the species are uncharged, should be about thermoneutral and hence have a very low energy barrier in the protein environment.

Taking into account possible polarizing effects of the protein on the energetics by the procedure described in Computational Methods, it was found that the barrier height of 8.8 kcal/mol at the B3LYP/6-31+G**//B3LYP/6-31+G* level was decreased by 1.7 kcal/mol to 6.1 kcal/mol, while the exothermicity of the conversion of the hydrogen-bonded reactant into the hydrogen-bonded product was increased by 0.2 kcal/mol to 4.4 kcal/mol.

With the free energy of activation of 14.7 kcal/mol obtained at the highest level, MP4(SDTQ)FC/6-31++G**//B3LYP/6-31+G* (see Table 7), the rate constant at 37 °C calculated^{33a} from the equation $k = (\kappa kT/2\pi\hbar) e^{-\Delta G^\ddagger/RT}$ is 44 s^{–1}.^{33b} Assuming that the same barrier height increment resulting from polarization effects is applicable to ΔG^\ddagger calculated at the highest level, the revised value for the rate constant at 37 °C is 700 s^{–1}. These two values thus lie on either side of the experimentally determined rate constant of 150 s^{–1} at 37 °C for the overall dehydration of the parent diol,³⁴ and strongly support the present model as a valid mechanism.

Comparison of the HO-Bridge, Fragmentation, Formic Acid Cofactor, and the Radical Cation Mechanisms. Reaction parameters calculated using E_c^0 , θ , and S^{298} data at the MP2(FC)/6-311++G**//MP2(FC)/6-31G* level reported in a previous paper, are listed in Table 8 for the dehydration of the 1,2-dihydroxyeth-1-yl radical via an HO-bridge structure (TS), and via fragmentation giving the HO radical and *syn*-vinyl alcohol; see reactions 2 and 3 in the Introduction. The rate-determining steps are respectively the formation of the transition state and the fission of the C–O bond; see Figure 9. Rate constants evaluated from the free energies of activation in the last column of the table, 26.0 and 21.8 kcal/mol, respectively, are given in Table 9, from which it can be seen that the values are far smaller than that for the formic acid cofactor mechanism by several powers of ten.

To be commensurate with the experimental value of 150 s^{–1} (for the overall dehydration of the diol radical)³⁴ the barrier heights would have to be diminished by about 12 and 8 kcal/mol, respectively. Such drastic reductions seem beyond any possible polarization effects of the protein, and unless some hitherto unexpected powerful influence is operative, we conclude that these two mechanisms are far less likely than either the formic and cofactor mechanism or proton transfer giving the 1,2-dihydroxyeth-1-yl radical cation, which has been found to undergo fission without activation. Some other completely different mechanism may, however, prove to be equally feasible.

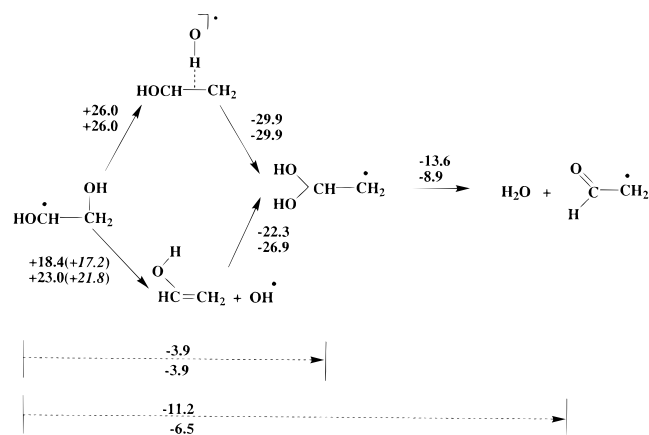


Figure 9. ΔG^{298} in kcal/mol, for the reaction steps in the gas phase (upper values) and at the active site of the enzyme (lower values) for the dehydration of the *cis*-1,2-dihydroxyethyl radical via an HO-bridge structure (transition state), reaction 2, and via a fragmentation process involving the formation of the HO radical and *syn*-vinyl alcohol, reaction 3, calculated at the MP2(FC)/6-311++G**//MP2(FC)/6-31G* level and (in parentheses) at the MP4(SDTQ)FC/6-31++G**//B3LYP/6-31+G* level.

TABLE 9: Rate Constants for the Dehydration of the 1,2-Dihydroxyethyl Radical in the Gas Phase, and at the Active Site, at 37 °C,^a Calculated from the ΔG^{298} Values in Tables 7 and 8 for Four Different Reaction Mechanisms (See Text)

mechanism	gas phase	active site ^b
HO-bridge (TS)	$4.8 \times 10^{-7} \text{ s}^{-1}$	$4.8 \times 10^{-7} \text{ s}^{-1}$
fragmentation	$7.7 \times 10^{-1} \text{ s}^{-1}$	$4.4 \times 10^{-4} \text{ s}^{-1}$
formic acid cofactor	44 s^{-1}	$44 (700) \text{ s}^{-1}$
radical cation	fast	fast

^a The experimentally determined rate constant for the dehydration of the parent diol 1,2-dihydroxyethane is 150 s^{-1} at 37 °C. ^b The value in parentheses takes into account a possible decrease in the enthalpy of activation of about 1.7 kcal/mol resulting from polarizing effects of the protein environment (see text).

Discussion

We note at the outset that neither the radical cation mechanism nor the carboxylic acid cofactor mechanism require the formation of the 1,1-diol as an obligatory intermediate in the dehydration process. As a consequence, neither mechanism is appropriate for the dehydration of 1,2-dihydroxypropane, since in this case ¹⁸O labeling experiments show unambiguously that the dehydration proceeds via the 1,1-diol. Nevertheless, both mechanisms remain as possibilities for the dehydration of 1,2-dihydroxyethane, and for the step in which water is eliminated in the ribonucleotide reductase reaction.

Both mechanisms are compatible with the absence of stereoselectivity in the dehydration of the (*R*)- and (*S*)-isomers of HOCHD-CH₂OH, the random (statistical) retention of the ¹⁸O label at the other carbon atom, and the absence of any exchange of the ¹⁸O label between the solvent H₂O and the acetaldehyde set free into solution.^{1b,c,d,f,g} The release of the formylmethyl radical as an independent intermediate, capable of rotation about the C-C bond, meets the requirement for racemization at both carbon atoms.

The hypothesis that interaction of the substrate (substrate radical) with an acidic group or with an acidic group and a basic group at the active site of the enzyme protein is an important element in the dehydration process and is one of long standing.^{1b,d,g} The radical cation mechanism and the carboxylic acid cofactor mechanism take this general hypothesis a necessary

step further by identifying the nature of the driving force in the dehydration process—namely, an inherent instability of the radical cation in the former mechanism, and a favorable reorganization of intermolecular hydrogen-bonding coupled with a complex redistribution of electronic charge in the latter.

The main difference between these two mechanisms lies in the role of the carboxylic acid H-atom. In the former, proton transfer yields the distonic radical cation³⁵ (H₂O⁺CH₂-CHOH), while in the latter the H-atom, along with the O-atom of the carbonyl group in the carboxylic acid, participates in intermolecular hydrogen-bonding. The primary dehydration product, the formylmethyl radical, (H₂C-CHO), is, however, the same in both mechanisms. There are also other similarities. In both mechanisms the O-atom of the water comes from the HOCH₂- group and not from the -CHOH group in the diol radical: thus, the O-atom in the carbonyl group of the formylmethyl radical, and hence the acetaldehyde, come from the -CHOH group in the diol radical. In both mechanisms the H-atoms of the water molecule originate in successive cycles of the dehydration process.³

We note that the many operational similarities between the radical cation and the carboxylic acid cofactor mechanism for the dehydration of the 1,2-dihydroxyethyl radical make it difficult to envisage an experimental procedure that could decide between them. The cofactor mechanism has the distinct advantage that bonding of the substrate radical at the active site is an *integral* feature in keeping with the oft-stated requirement to explain the results of stereochemical and inhibitor studies.^{1g} With the radical cation mechanism, on the other hand, substrate radical bonding would have to be introduced as an *ancillary* feature.

Finally, the finding that the substrate itself forms a nine-membered hydrogen-bonded ring structure with formic acid, like the substrate radical, shows that bonding at the active site prior to H-atom transfer to the 5'-deoxyadenosyl radical is entirely feasible. This initial step would be in accord with the long-accepted hypothesis that two-point attachment of the substrate to the enzyme protein via the HO-groups of the diol is an essential feature of the dehydrase reaction.^{1g} The difference lies in that with a carboxylic acid group as the attachment site, once H-atom transfer has occurred the dehydration process would proceed unaided.

Acknowledgment. We thank the Advanced Scientific Computing Laboratory, NCI-FCRF, for providing time on the CRAY YMP supercomputer. The authors would also like to acknowledge the technical support provided by Carol Afshar. This work was supported by Grants CA-10925 and CA-06927 from the National Institutes of Health and by an appropriation from the Commonwealth of Pennsylvania. Its contents are solely the responsibility of the authors and do not necessarily represent the official views of the National Cancer Institute.

Supporting Information Available: Table 1S: S^{298} , the entropies in kcal/(mol K), zpe , the zero-point energies in hartrees, and θ , the total thermal energies at 298 K in hartrees, evaluated from vibrational frequencies calculated at the B3LYP/6-31+G**//B3LYP/6-31+G* level: E_e^0 , the ground-state electronic energies at 0 K, in hartrees, calculated at the B3LYP/6-31+G**//B3LYP/6-31+G* level (upper values) and at the MP2(FULL)/6-311++G(2d,2p)/6-31+G* level (lower values), together with E^{298} , the total molecular energies at 298 K—the sum of E_e^0 and θ . **Table 2S:** Ground-state electronic energies at 0 K, E_e^0 , in hartrees, calculated at the MP4(SDTQ)FC/6-

31++G**//B3LYP/6-31+G* level, with additional values (in italics) for the hydrogen-bonded reactant, the transition state, and the hydrogen-bonded product calculated at the MP4(SDTQ)-FC/6-31++G**//B3LYP/6-31++G** level. **Table 3S:** The entropy, S^{298} , cal/(mol K) for the ideal gas state, the individual contributions from translation, rotation, vibration and electronic entropy, and the internal entropy given by the sum $S_{\text{int}}^{298} = S_{\text{int}}^{298} + S_{\text{vib}}^{298} + S_{\text{elec}}$ calculated at the B3LYP/6-31+G**//B3LYP/6-31+G* level, together with estimated values for the liquid state using the empirical equation $S_{\text{liq}} = 15.8 + S_{\text{int}}^{298}$. **Table 4S:** As in Table 3S but with the values calculated at the MP2(FC)/6-31+G**//MP2(FC)/6-31+G* level. This material is available free of charge via the Internet at <http://pubs.acs.org>.

References and Notes

- (1) (a) Babior, B. M. *Acc. Chem. Res.* **1975**, *8*, 376–384. (b) Abeles, R. H.; Dolphin, D. *Acc. Chem. Res.* **1976**, *9*, 114–120. (c) Abeles, R. H. In *Vitamin B₁₂, Proceedings of the Third European Symposium on Vitamin B₁₂ and Intrinsic Factor*, University of Zurich, March 5–8, 1979, Zurich, Switzerland; Zagalak, B., Friedrich, W., Eds.; Walter De Gruyter: Berlin, 1979; pp 373–388. (d) Arigoni, D. As in (c), pp 389–411. (e) Golding, B. T. In *Chemistry, B₁₂*; Dolphin, D., Ed.; Wiley-Interscience: New York, 1982; Vol. 1, *Chemistry*, Chapter 15, pp 543–582. (f) Rétey, J. In *Stereochemistry*; Tamm, C. H., Ed.; Elsevier: Biomedical Press: Amsterdam, 1982; Chapter 6. (g) Finke, R. G.; Schiraldi, D. A.; Mayer, J. M. *Coord. Chem. Rev.* **1984**, *54*, 1–22. (h) Dixon, R. M.; Golding, B. T.; Mlwesigye-Kibende, S.; Ramakrishna Rao, D. N. *Philos. Trans. R. Soc. London* **1985**, *B311*, 531–544. (i) Halpern, J. *Science* **1985**, *277*, 869–875. (j) Golding, B. T.; Buckel, W. Corrin-Dependent Reactions: In *Comprehensive Biological Catalysis*; Sinnott, M., Ed.; Academic Press: New York, 1998; Vol. III, Chapter 33, pp 239–259 (see also references therein).
- (2) Golding, B. T.; Radom, L. *J. Am. Chem. Soc.* **1976**, *98*, 6331–6338.
- (3) George, P.; Glusker, J. P.; Bock, C. W. *J. Am. Chem. Soc.* **1997**, *119*, 7065–7074.
- (4) Russell, J. J.; Rzepa, H. S.; Widdowson, D. A. *J. Chem. Soc., Chem. Commun.* **1983**, 625–627.
- (5) (a) Stubbe, J. *Adv. Enzymol. Relat. Areas Mol. Biol.* **1989**, *63*, 349–417. (b) Stubbe, J. *J. Biol. Chem.* **1990**, *265*, 5329–5332.
- (6) Siegbahn, Per E. M. *J. Am. Chem. Soc.* **1998**, *120*, 8417–8429.
- (7) Bertini, F.; Caronna, T.; Grossi, L.; Minisci, F. *Gazz. Chim. Ital.* **1974**, *104*, 471–478.
- (8) Frisch, M. J.; Trucks, G. W.; Schlegel, H. B.; Gill, P. M. W.; Johnson, B. G.; Robb, M. A.; Cheeseman, J. R.; Keith, T.; Petersson, G. A.; Montgomery, J. A.; Raghavachari, K.; Al-Laham, M. A.; Zakrzewski, V. G.; Ortiz, J. V.; Foreman, J. B.; Cioslowski, J.; Stefanov, B. B.; Nanayakkara, A.; Challacombe, M.; Peng, C. Y.; Ayala, P. Y.; Chen, W.; Wong, M. W.; Andres, J. L.; Repogle, E. S.; Gomperts, R.; Martin, R. L.; Fox, D. J.; Binkley, J. S.; Defrees, D. J.; Baker, J.; Stewart, J. P.; Head-Gordon, M.; Gonzalez, C.; Pople, J. A. Gaussian 94, Revision E.2; Gaussian Inc.: Pittsburgh, PA, 1995.
- (9) (a) Becke, A. D. *Phys. Rev.* **1988**, *A38*, 3098. (b) Becke, A. D. *J. Chem. Phys.* **1993**, *98*, 1372. (c) Becke, A. D. *J. Chem. Phys.* **1993**, *98*, 5648. (d) Lee, C.; Yang, W.; Parr, R. G. *Phys. Rev.* **1988**, *B37*, 785. (e) Vosko, S. H.; Wilk, L.; Nusair, M. *Can. J. Phys.* **1980**, *58*, 1200. (f) Perdew, J. P.; Wang, Y. *Phys. Rev. B* **1992**, *45*, 13244. (g) Perdew, J. P. In *Electronic Structure of Solids*; Ziesche, P., Eischrig, H., Eds.; Akademie Verlag: Berlin, 1991. (h) Perdew, J. P.; Chevary, J. A.; Vosko, S. H.; Jackson, K. A.; Pederson, M. R.; Singh, D. J.; Fiolhais, C. *Phys. Chem. B* **1992**, *46*, 6671.
- (10) Reed, A. E.; Weinstock, R. B.; Weinhold, F. *J. Chem. Phys.* **1985**, *83*, 735–746.
- (11) (a) McIver, J. W., Jr.; Kormornicki, A. *J. Am. Chem. Soc.* **1972**, *94*, 2625–2633. (b) Pople, J. A.; Krishnan, R.; Schlegel, H. B.; Binkley, J. S. *Int. J. Quantum Chem. Symp.* **1979**, *13*, 225–241. (c) Schlegel, H. B. In *New Theoretical Concepts for Understanding Organic Reactions*; Bertran, J., Csizmadia, I. G., Eds.; Kluwer: Academic Publishers: Dordrecht, The Netherlands, 1989; pp 33–53.
- (12) (a) Hariharan, P. C.; Pople, J. A. *Theor. Chim. Acta* **1973**, *28*, 213–222. (b) Binkley, J. S.; Pople, J. A. *Int. J. Quantum Chem.* **1975**, *9*, 229–236. (c) Möller, C.; Plesset, M. S. *Phys. Rev.* **1934**, *46*, 618–622. (d) Pople, J. A.; Binkley, J. S.; Seeger, R. *Int. J. Quantum Chem. Symp.* **1976**, *10*, 1–19.
- (13) Del Bene, J. E. In *Molecular Structure and Energetics*; Liebman, J. F., Greenberg, A., Eds.; VCH Publishers: Deerfield Beach, FL, 1986; Vol. 1, Chapter 9.
- (14) (a) Wiberg, K. B.; Rablen, P. R.; Rush, D. J.; Keith, T. A. *J. Am. Chem. Soc.* **1995**, *117*, 4261–4270. (b) Wiberg, K. B.; Keith, T. A.; Frisch, M. J.; Murcko, M. *J. Phys. Chem.* **1995**, *99*, 9072–9079.
- (15) Blomberg, M. R. A.; Siegbahn, P. E. M.; Babcock, G. T. *J. Am. Chem. Soc.* **1998**, *120*, 8812–8824.
- (16) Stull, D. R.; Westrum, E. F., Jr.; Sinke, G. C. *The Chemical Thermodynamics of Organic Compounds*; John Wiley and Sons: New York, 1969.
- (17) Powell, R. E.; Latimer, W. M. *J. Chem. Phys.* **1951**, *19*, 1139–1141.
- (18) Cobble, J. W. *J. Chem. Phys.* **1953**, *21*, 1451–1456.
- (19) Values of ϕ in the equation $\phi = S_{\text{liq}} - S_{\text{int}}^{298}$ calculated for molecules with N “skeletal” bonded atoms, and the number of examples (in parentheses) in each case: $N = 3$, 17.0 ± 1.7 (8); $N = 4$, 16.6 ± 1.8 (14); $N = 5$, 17.0 ± 1.3 (31); $N = 6$, 16.0 ± 1.5 (23); $N = 7$, 16.4 ± 1.0 (24); $N = 8$, 15.5 ± 1.3 (36); $N = 9$, 13.2 ± 0.7 (11); $N = 10$, 13.3 ± 1.2 (14).
- (20) Wellington Davis, R.; Robiette, A. G.; Gerry, M. C. L.; Bjarnov, E.; Winnewisser, G. *J. Mol. Spectrosc.* **1980**, *81*, 93–109.
- (21) Cook, R. L.; De Lucia, F. C.; Helsing, P. *J. Mol. Spectrosc.* **1974**, *53*, 62–76.
- (22) Kibb, R. W.; Lin, C. C.; Wilson, E. B. *J. Chem. Phys.* **1957**, *26*, 1695–1703.
- (23) Latimer, W. M. *The Oxidation States of the Elements and Their Potentials in Aqueous Solution*, 2nd ed.; Prentice-Hall: New York, 1956; pp 39 and 128.
- (24) Levine, I. N. *Physical Chemistry*, 4th ed.; McGraw-Hill: New York, 1995; p 843.
- (25) Bock, C. W.; Trachtman, M.; George, P. *J. Mol. Spectrosc.* **1980**, *80*, 131–144.
- (26) Pedley, J. B.; Naylor, R. D.; Kirby, S. P. *Thermochemical Data of Organic Compounds*, 2nd ed.; Chapman and Hall: London, 1986.
- (27) (a) Hocking, W. H. *Z. Naturforsch.* **1976**, *A31*, 1113–1121. (b) Bjarnov, E.; Hocking, W. H. *Z. Naturforsch.* **1978**, *A33*, 610–618.
- (28) (a) Van Alsenoy, C.; Van den Enden, L.; Schäfer, L. *J. Mol. Struct. (THEOCHEM)* **1984**, *108*, 121–128. (b) Murcko, M. A.; DiPaola, R. A. *J. Am. Chem. Soc.* **1992**, *114*, 10010–10018. (c) Oie, T.; Topol, I. A.; Burt, S. K. *J. Phys. Chem.* **1994**, *98*, 1121–1128.
- (29) Garrett, B. C.; Truhlar, D. G. *J. Phys. Chem.* **1979**, *83*, 200–203.
- (30) (a) Pimental, G. C.; McClellan, A. L. *The Hydrogen Bond*; W. H. Freeman and Co.: San Francisco and London, 1960 (see also references therein). (b) Olovsson, I.; Jonsson, P.-G. *The Hydrogen Bond*; North-Holland: Amsterdam, The Netherlands, 1976. (c) Jeffrey, G. A. *An Introduction to Hydrogen Bonding*; Oxford University Press: New York, Oxford, 1997.
- (31) In a planar nine-membered ring the sum of the ring angles is 1260° : but if two are approximately 180° the sum of the remaining angles would be about 900° —on average about 129° . This far exceeds the equilibrium values for any of the angles around the ring, $\angle\text{OCC}$, $\angle\text{CCO}$, $\angle\text{COH}$, and $\angle\text{OCO}$, so a marked departure from planarity is unavoidable in order to reduce the strain.
- (32) (a) George, P.; Bock, C. W.; Trachtman, M. *J. Mol. Struct. (THEOCHEM)* **1983**, *92*, 109–139. (b) George, P.; Bock, C. W.; Trachtman, M. *J. Mol. Struct. (THEOCHEM)* **1985**, *133*, 11–24. (c) George, P.; Bock, C. W.; Trachtman, M. *J. Mol. Struct. (THEOCHEM)* **1987**, *152*, 35–53.
- (33) (a) Kondratiev, V. N.; Nikitin, E. E. *Gas-Phase Reactions*; Springer-Verlag: New York, 1981; pp 60 and 104. (b) Assuming the transmission coefficient κ to be unity and substituting numerical values for Boltzmann’s constant and Planck’s constant, this equation reduces to $k = 1.03 \times 10^{12} e^{-\Delta G^\ddagger/RT} \text{ s}^{-1}$ for 37°C .
- (34) Bachovchin, W. W.; Eager, R. G., Jr.; Moore, K. W.; Richards, J. H. *Biochemistry* **1977**, *16*, 1082–1092.
- (35) Yates, B. F.; Bouma, W. J.; Radom, L. *J. Am. Chem. Soc.* **1984**, *106*, 5805–5808.